TECHNICAL MEMORANDUMS

NATIONAL ADVISORY COMMITTEE FOR AERONAUTICS

No. 951



# VARIATION IN VELOCITY PROFILE WITH CHANGE IN SURFACE ROUGHNESS OF BOUNDARY

By W. Jacobs

Zeitschrift für angewandte Mathematik und Mechanik
Vol. 19, No. 2, April 1939

Washington
September 1940

NATIONAL ADVISORY COMMITTEE FOR AERONAUTICS

---

TECHNICAL MEMORANDUM No. 951

---

# VARIATION IN VELOCITY PROFILE WITH CHANGE IN SURFACE ROUGHNESS OF BOUNDARY*

By W. Jacobs

## SUMMARY

The present report deals with the variation of a turbulent velocity profile in flow from rough to smooth wall and vice versa. Expressions obtained for the shear-stress distribution with respect to the distance from the point of junction of the different roughnesses and from the wall distance, are utilized to ascertain the developing velocity distributions. Under simplified assumptions, the use of these formulas renders possible the integration of the motion equations for the shear stress. This calculation is carried out and compared with the experiments. Despite the fact that the assumptions in this particular case do not prove to be wholly correct, comparatively good agreement is achieved in the most important region.

## INTRODUCTION

The purpose of this report is to study the variation of a turbulent velocity profile established in a channel of known surface roughness on transition to a different surface roughness by experiments, and to develop the formulas necessary for the calculation. The phenomena accompanying fully established flow along a boundary of known roughness may be considered as being understood now (reference 1). Expressions have been obtained for smooth and

---

*"Umformung eines turbulenten Geschwindigkeitsprofiles." Zeitschrift fur angewandte Mathematik und Mechanik, vol. 19, no. 2, April 1939, pp. 87-100.
This article forms the second part of the thesis, under the direction of Professor Prandtl, entitled: "Studien zum Rauhigkeitsproblem." The first part, entitled: "Strömung hinter einem einzelnen Rauhigkeitselement," appeared in Ing.-Arch., vol. IX, no. 5, 1938, p. 343.

rough tubes and channels for the velocity distribution, resistance, exchange in impulse, and the mixing path. If the surface roughness undergoes a change, a new velocity profile has to be formed, and this transition region has, so far, been investigated only theoretically, under certain simplifying assumptions (reference 2). The author has carried out experiments over this region and utilized the results to establish a new method for computing the velocity distribution over the transition section of a channel when changing from smooth to rough, and vice versa, provided the shear stress at the wall under conditions of fully established flow, is known. The predictions have been confirmed by further experiments.

## EXPERIMENTAL SET-UP

Experiments were carried out on a blower whose nozzle emptied into a rectangular channel 60 cm wide and 20 cm high. The channel itself consisted of airtight wooden boxes, bolted together with felt strips in between, insuring a completely closed channel length which could be lengthened or shortened as necessity arose. The end of the channel formed the experiment chamber. Glass windows on the side assured the most accurate setting of the pitot tubes. In virtue of the reflection on the smooth wall, an accuracy up to 1/10 mm was readily obtainable for a known point of contact of the survey tube with the wall and hence, of the wall distance. The experiment chamber itself was so arranged that the survey tube could be moved across the entire length of the box but not crosswise to the direction of flow (fig. 1). The box was 1.5 m long.

Above it was the guide rail of an optical bench, to which the streamlined tube was fastened. The survey tubes were fitted with threads and laterally screwed to the streamlined tube. The recorded pressure was transmitted by means of a valve rubber to a little tube inside the streamlined tube and was removable from above. The slot in the upper wall was covered during the test by well-fitting wooden strips.

Since a two-dimensional problem was involved, the static pressure could be recorded with a disk type of survey tube originally employed by Motzfeld (reference 3), consisting of a lens-shaped disk of 8 mm diameter, 1 mm maximum thickness, with 0.6 mm diameter orifices in the

center of the curved surfaces. The survey tube should be so introduced that the mean flow direction is always parallel to the tube. The directional unsusceptibility was approximately $\pm 3^{\circ}$ and was at any time obtainable. A calibration was made in the free stream, back of the fan, in the "sound" flow, with the static pressure set at zero. The coefficients were almost identical with the employed survey tubes, averaging around $\beta = 1.14$. This value was largely independent of the Reynolds number. With the notation:

$p_g$ total pressure

$p_{st}$ static pressure

$p_{st}'$ static pressure recorded by the survey tube

$q$ dynamic pressure

We have:

$$p_g - p_{st}' = \beta q$$

$$p_{st} = p_g - q = p_g - \frac{p_g - p_{st}'}{\rho} = \frac{1}{\beta}\left[(\beta - 1)\, p_g + p_{st}'\right]$$

which, with $\beta = 1.14$, gives the static pressure at

$$p_{st} = \frac{0.14\, p_g + p_{st}'}{1.14}$$

All pressures were recorded with Prandtl manometer relative to the pressure in the experiment chamber. Strips 0.7 cm high and 1.0 cm wide, nailed 15 cm apart on the bottom side of the channel, simulated the wall roughness. The rough length amounted to 5 m.

## PRELIMINARY TESTS

Before proceeding to the actual measurements, it was necessary to ascertain whether a fully established pro-

file existed at the end of the rough length. Plotting the velocity against the logarithm of the wall distance, gave a straight line which, according to the logarithmic law of velocity distribution, is an indication of fully developed flow, as was to be expected on the basis of Nikuradse's earlier pipe flow experiments, which established the termination of mixing after about 40 pipe radii. Kirsten (reference 4) claims the presence of the final velocity distribution at 20 pipe radii already. With a hydraulic radius of

$$r_h = \frac{2 \text{ channel section}}{\text{with circumference}} = 15 \text{ cm}$$

in our case we obtain a distance of 33.3 radii available as entrance which, considering the marked roughness, should be sufficient for full development of the profile.

The measurement of the pressure drop was accompanied by a slight pressure jump behind the roughnesses, on transition to the smooth wall, caused by the abrupt widening of the channel. A smooth, carefully alined plywood board, high enough to assure progressive transition of the pressure, was nailed at the smooth part of the length. If the board was too thick, naturally the opposite occurred: a pressure jump to too small values. After various trials, 1.0 cm was chosen as a practical height.

The static pressure drop records were made in the middle of the channel. The effect of v, that is, of the velocity perpendicular to the wall, on the pressure reading, was below the accuracy limit; hence, could be disregarded. For, with $p'_{st_v}$ as the additional pressure indicated by v, our calibration above affords:

$$p'_{st_v} - p_{st}' = - 0.14 \frac{\rho}{2} v^2, \quad p_{st}' - p_{st} = 0.14 \frac{\rho}{2} u^2$$

Assuming roughly that v/u in the center acts as 1:100 - this value is not reached in our case - we have:

$$\frac{p'_{st_v} - p_{st}'}{p_{st}' - p_{st}} = \frac{1}{10000}$$

The omission is therefore fully justified.

The slight irregularity of the velocity distribution across the width of the channel, was of no import in these tests as the measurements were made in a vertical plane.

## TEST PROCEDURE

Having to do with a two-dimensional problem, the x-y coordinates are formed by the perpendicular plane of symmetry of the channel in the flow direction, its zero point being situated in the junction point of the two roughnesses. The positive x axis points in the direction of the principal flow; the positive y axis, perpendicularly upward.

The flow was studied when changing from smooth to rough wall and vice versa. However, for reasons evolving from the experiments, only the variation in the profile from rough to smooth, is to be analyzed in detail. Velocity measurements were made at $x = 2$, 7, 15, 20, 40, 70, 100, 150, 215, and 290 cm (fig. 2), although only part of the obtained curves are shown, for the sake of clarity. The variation in the profile is such that in the lower regions with increasing $x$, an increase - and in the middle a decrease - in velocity occurs, whereby the smooth profile evolves gradually. This transition is numerically treated.

## ATTEMPTED SOLUTION

With $\tau$ = apparent shear stress, the equation of motion reads:

$$u \frac{\partial u}{\partial x} + v \frac{\partial u}{\partial y} = - \frac{1}{\rho} \frac{\partial p}{\partial x} + \frac{1}{\rho} \frac{\partial \tau}{\partial y}$$

With the continuity equation $\frac{\partial u}{\partial x} + \frac{\partial v}{\partial y} = 0$, we obtain, conformable to a variation by Prandtl (reference 5):

$$- u \frac{\partial v}{\partial x} + v \frac{\partial u}{\partial y} = - \frac{1}{\rho} \frac{\partial p}{\partial x} + \frac{1}{\rho} \frac{\partial \tau}{\partial y} = f(y)$$

where, for a fixed $x$, the right-hand side is put equal to a function of $y$; or

$$-\frac{\partial}{\partial y}\left(\frac{v}{u}\right) = \frac{-u\frac{\partial v}{\partial y} + v\frac{\partial u}{\partial y}}{u(y)^2} = \frac{f(y)}{u(y)^2}$$

We integrate from 0 to y, since $v = 0$ for $y = 0$,

$$\frac{v}{u} = -\int_0^y \frac{f(y)}{u(y)^2}\,dy \quad \text{and hence,} \quad v = -u\int_0^y \frac{f(y)}{u(y)^2}\,dy$$

whence differentiation gives the velocity increase:

$$-\frac{\partial v}{\partial y} = +\frac{\partial u}{\partial x} = \frac{\partial}{\partial y}\left(u\int_0^y \frac{f(y)}{u(y)^2}\,dy\right)$$

Starting therefore from a certain velocity profile, if $\frac{\partial p}{\partial x}$ (which in first approximation can be put constant because of the small curvature of the streamlines over the channel section) and $\frac{\tau}{\rho}$ are known, $\frac{\partial u}{\partial x}$ can be computed, wherefrom follows a new $u$ for $(x + \Delta x)$:

$$u_2 = u_1 + \left(\frac{\partial u}{\partial x}\right)_1 \Delta x$$

The method applied recurrently gives, therefore, the velocity distributions at the various distances. For the shear stress, the formula

$$\frac{\tau}{\rho} = l^2 \left|\frac{\partial u}{\partial y}\right| \frac{\partial u}{\partial y} \quad \text{(reference 6)}$$

was applied. It could be computed under rough assumptions of mixing path $l$. Reliable mixing-path distributions in a channel are unknown. Hence, the use of the simple formula $l = 0.4\,y\,\frac{h - y}{h}$, which for $y = \frac{h}{2}$ gives $l = 0.1\,h$ (fig. 3); $h$ = channel height.

The calculation was then attempted with this assump-

tion. The velocity u of the initial profile supplied the measurement, $\frac{\partial u}{\partial y}$ had to be defined graphically by differentiation. The result was the shear stress and after another differentiation $\frac{\partial \tau}{\partial y}$. The integral $\int_0^y \frac{f(y)}{u(y)^2} dy$ was graphically evaluated. Reiterated differentiation of $u \int_0^y \frac{f(y)}{u(y)^2} dy$ finally gave the desired velocity difference for the selected path element $\Delta x$.

Notwithstanding the various applications of the usually not too-accurate differentiation and graphical integration, we still believed that with the care used, the results would agree with the actual conditions; but it was otherwise. A comparison with the experimentally ascertained velocities manifested, to be sure, close agreement for greater distances from the wall, but also great departures in the neighborhood of the wall. The advance of the rough profile toward the smooth, up to y values of several centimeters, took place much faster than the calculation stipulated. The reason could only be ascribed to the erroneous mixing-path assumptions.

In the attempted explanation of these conditions, the opposite process was essayed - that is, the shear stress was computed from the recorded velocity profiles and their differences, and the extent to which the above functional relation of mixing path and y was true or false, and was independent of x, was checked by means of the formula $\frac{\tau}{\rho} = l^2 \left|\frac{\partial u}{\partial y}\right| \frac{\partial u}{\partial y}$. The equations of motion and continuity served as basis.

The result definitely established the reason for the discrepancies between calculation and experiment, and made the continuation of the above method appear little promising. The rise of the mixing path with the distance from the wall was much more pronounced than we had stipulated

in our formula, according to Nikuradse's experiments on pipe friction. But at greater x values (150-200 cm) - that is, on approaching the fully established smooth profile of Nikuradse's distribution, the mixing-path distribution was approximately similar (it was a little below).

Incidentally, it may be mentioned that, according to Prandtl, the mixing path on approaching the wall tends toward a certain limiting value, which corresponds to the degree of roughness. This value, being small, was disregarded in our calculations. To illustrate: Consider our utilized rough wall; writing, in conformity with the universal law of velocity distribution for rough walls (Nikuradse, reference 1),

$$8.5 + 5.75 \log \frac{y_o}{k_s} = \frac{u}{v_{*_r}} = 0$$

gives the wall distance $y_o$, with velocity = zero, according to our law. $v_{*_r}$ is the shear stress and $k_s$ the equivalent grain size, which will be determined later. Assuming its value for the present, gives:

$$\log \frac{y_o}{k_s} = \log \frac{y_o}{5.26} = -\frac{8.5}{5.75}, \quad y_o = 0.175 \text{ cm}, \quad l_o = 0.068 \text{ cm}$$

This value $l_o$ would not have been able to change the mixing path distribution very much. On the smooth channel wall used it was, in fact, several percent lower, so that it could not be considered at all. The wide discrepancies therefore remained unexplained; hence the solution of the posed problem by this method must be called unsuccessful.

## FORMULATION OF AN EMPIRICAL SHEAR STRESS DISTRIBUTION FORMULA

a) Determination of wall shear stresses and closer characterization of wall roughness.- Before going on with the new method, the utilized roughness and its shear stresses are scrutinized somewhat more closely.

$\tau_g$ is the shear stress on the smooth wall; $\tau_r$ that

on the rough wall. $\tau_g$ was obtained once by pressure drop, at $\frac{\tau_g}{\rho} = 4.90 \times 10^3 \text{ cm}^2/\text{s}^2$. But since this value seemed too uncertain, the determination of $\tau_g$ by the universal law of velocity distribution:

$$\frac{u}{v_{*_g}} = 5.5 + 5.75 \log \frac{v_{*_g} y}{\nu}$$

served as check. Logarithmic plotting of the wall distance $y$ against the velocity $u$ affords a straight line

$$u = m_g + n_g \log y$$

from whose slope $v_{*_g}$ follows direct

$$n_g = 5.75\, v_{*_g}, \qquad v_{*_g} = \sqrt{\frac{\tau_g}{\rho}} = \frac{n_g}{5.75}$$

It gave:

$$\frac{\tau_g}{\rho} = 5.05 \times 10^3 \text{ cm}^2/\text{s}^2$$

The factor 5.75 was considered safe. The two obtained values agreed fairly closely. The additive constant of 4.32 in our universal velocity distribution law differing from Nikuradse's 5.5, is attributable to the fact that the wall is not perfectly smooth. Thus the universal law for our case reads:

$$\frac{u}{v_{*_g}} = 4.32 + 5.75 \log \frac{v_{*_g} y}{\nu}$$

The slope of the straights is the same as Nikuradse's.

With $a$ = side length, $b$ = height of the channel section, $\tau_r/\rho$ is now computed from the force equilibrium between wall shear stress and pressure gradient:

$$\frac{\tau_r}{\rho} a + \frac{\tau_g}{\rho} (a + 2b) = \frac{a\, b}{\rho} \frac{dp}{dx}$$

$$\frac{\tau_r}{\rho} = \frac{b}{\rho} \frac{ap}{ax} - \frac{\tau_g}{\rho} \left(1 + \frac{2b}{a}\right) = 22.2 \times 10^3 \text{ cm}^2/\text{s}^2$$

Analogous to the determination of $\tau_g/\rho$, $\tau_r/\rho$ can now be obtained for checking the last-obtained value. For a rough wall, the universal velocity distribution law takes the form

$$\frac{u}{v_{*_r}} = A + 5.75 \log \frac{y}{k_s}, \qquad u = m_r + n_r \log y$$

which, plotted as previously, leaves

$$\sqrt{\frac{\tau_r}{\rho}} = v_{*_r} = \frac{n_r}{5.75} = 155 \text{ cm/s}, \qquad \frac{\tau_r}{\rho} = 24.1 \times 10^3 \text{cm}^2/\text{s}^2$$

Even in this case, the values are fairly agreeable. With the approximate average value $\frac{\tau_r}{\rho} = 23.0 \times 10^3$ $\text{cm}^2/\text{s}^2$ were computed.

It should be noted that the roughness of the board used for the cross-sectional contraction, was slightly different from the channel wall. This explains the difference between the above-defined wall shear stress, applicable for the usual channel wall, and that later obtained as constant after integration of $\frac{1}{\rho}\int_0^y \frac{\partial \tau dy}{dy}$, which represents the shear stress of the board. This value ranged from $\frac{\tau}{\rho} = 3 \times 10^3$ to $4 \times 10^3$ $\text{cm}^2/\text{s}^2$. Subsequently, $3.4 \times 10^3$ was used in the calculation, as it involved flow conditions over the "smooth" board.

At this time, a remark about the shear stress on the smooth wall when facing the rough wall, may not be amiss. From the smallness of the discrepancies appearing in the measurements, it may be concluded that in this case the wall shear stress is greater than when the whole channel is smooth. The roughness effect extends across the entire channel width up to the opposite wall.

For comparing our roughness with that of others, we effected a reduction to Nikuradse's grain size, although this should not be looked upon as generally the best ref-

erence roughness. One of Schlichting's grain sizes (reference 7) might perhaps be more appropriate since in Nikuradse's roughness - because of the adhesion of the sand grains with lacquer - the conditions between the grains cannot be accurately simulated.

The equivalent grain size gives the grain size of Nikuradse's sand roughness, having the same resistance as the roughness used; it is indicated by $k_s$. The universal velocity distribution law for rough wall for fully established flow, reads:

$$\frac{u}{v_{*_r}} = A + 5.75 \log \frac{y}{k}$$

A is characteristic of any roughness; it is a roughness function. For sand roughness, the value is $A_s = 8.48$. Accordingly,

$$\frac{u}{v_{*_r}} = 8.48 + 5.75 \log \frac{y}{k_s}$$

and, comparison with the preceding relation:

$$8.48 + 5.75 \log \frac{y}{k_s} = A + 5.75 \log \frac{y}{k}$$

or, after combining:

$$5.75 \log \frac{k_s}{k} = 8.48 - A$$

Semilogarithmic plotting gives, in our case, $A = 3.45$. Hence,

$$\log \frac{k_s}{k} = 0.876, \qquad \frac{k_s}{k} = 7.52$$

which, for the $k = 0.7$ cm height of roughness used, amounts to

$$k_s = 5.26 \text{ cm}$$

The size of the equivalent sand roughness is therefore $7\frac{1}{2}$ times greater than that of the used roughness.

Further calculation demands an exact definition of the wall distance. Schlichting defined it as equal to the distance of a fictitious wall substituting for the rough wall, having the same fluid volume. This was found to be impractical. The starting point formed the logarithmic velocity-distribution law:

$$u = 5.75\ v_* \log \frac{y}{y_o}$$

$\log \frac{y}{y_o}$ was then plotted against $u$, while $y_o$ was varied until the extension of the obtained straight lines passed through zero. The points adjacent to the wall were omitted, since the law does not apply there. The thus-obtained point $y_o$ represents the height at which the velocity is zero, and consequently, forms the zero point of the new coordinate system. $y_o$ was equal to 0.17 cm. This agrees with Nikuradse's definition, according to which $y_o = \frac{k_s}{30}$. In our case $y_o = \frac{5.26}{30}\ k = 0.175\ k$.

The velocity measurements were made at an average air speed of around 14 m/s. The velocity (16.40 m/s) recorded in the middle of the channel served to effect the nondimensionality.

b) Mathematical shear stress distribution.- Reverting to our original problem - that is, the calculation of the variation in velocity profile - it was necessary to obtain some kinds of expressions. A ray of light in this direction was indicated during the plotting of the shear stresses computed from the experiment. The shear stress by fully established flow is, as known, linearly distributed across the section. It is zero at maximum velocity and increases with approach to the wall up to the corresponding wall shear stress. The shear stresses prevailing at different distances from the roughness transition point, were all between the linearly rough and smooth distribution, working from the rough with increasing $x$ over to the smooth (fig. 4). The new wall shear stress was immediately available. Its effect spread consistently upward. Hence, it was presumed that the differences between the original rectilinear shear stress distribution and that existing at certain distances, might be approximately expressible by an exponential relationship between $y$ and $x$. Comparisons of various formulas with the obtained shear stress distribution, manifested the following as the most favorable:

$$\tau(x,y) = [\tau_r - (\tau_r - \tau_g) f(\eta)]\frac{h - y}{h} \qquad (1)$$

$$f(\eta) = a\, e^{-b\eta} \quad \text{with} \quad \eta = \frac{y}{x^m} \qquad (2)$$

$y = h$ indicates the ordinate of the maximum velocity. For fully established smooth and rough flow, $h$ assumes, of course, different values - a fact which was not taken into consideration, as its role is subordinate in our analysis. A certain compensation might be achieved by resorting to the arithmetic mean of the height as basis of the calculation. Our choice on transition from rough to smooth as height $h$ is the distance of the velocity maximum on the rough profile from the wall.

During the closer investigation of our previous surmise $f(\eta)$ was first plotted from equation (1) against $y$ for different $x$ (fig. 5):

$$f(\eta) = 1 + \frac{\tau_g}{\tau_r - \tau_g} - \frac{\tau(x,y)}{\tau_r - \tau_g}\frac{h}{h - y}$$

A certain value $f(\eta) = a\, e^{-by/x^m} = \text{constant}$ defines a certain value $\eta = \frac{y}{x^m} = \text{constant}$. Therefore,

$$\ln y = \ln \text{const} + m \ln x$$

After logarithmic plotting of $y$ and $x$, followed by the drawing of straight lines through the points obtained for $f(\eta) = \text{const}$ - the errors encountered being compensated for as much as possible - their slope $m$ indicates the exponent of $x$ (fig. 6). The gratifying feature of our formula (above) is that with it the average slope of the straight lines was quite constant; i.e., approximately equal to 1, in consequence of which $f(\eta)$ assumed a form easily amenable to calculation. $\eta$ forms the intersection on the ordinate obtained by extension of the straight line placed as closely as possible through the points with the averaged slope 1 as far as the intersection with the ordinate axis.

There remained the determination of $a$ and $b$:

$$f(\eta) = a\, e^{-b\frac{y}{x}}, \qquad \log[f(\eta)] = \log a - b\,\eta$$

Semilogarithmic plotting then gave a and b. For a we obtained about 1, as it should be, if $\tau_{(xy)} = \tau_g$ for small y; for b, we obtained 11.16 (fig. 7).

Then, the general relationship of x and y for $\tau$ reads:

$$\tau_{(xy)} = \left[ \tau_r - (\tau_r - \tau_g)\, e^{-11.16 \frac{y}{x}} \right]^{\frac{h-y}{h}} \qquad (3)$$

This is an empirically established formula for the change in shear stress distribution on transition from rough to smooth wall.

Now it remained to be proved, to what extent a generalization of this formula was permissible to other cases. For this purpose, the investigations were made by exactly opposite conditions, as in flow from smooth to rough wall. The length intended as entrance obtained a bottom support of 1 cm thickness, of the same boards used in the first test and, consequently, with exactly the same roughness. The entrance length of 5 m was considered sufficient for establishing the profile.

Next comes a rough length of about 3 m. Great care was used in fastening the board on the bottom, so as to obtain a perfect plane and keep the cross-sectional changes within negligible limits. The smooth piece was followed by the strips spaced at the given distances. The measurements were made in the exact center between strips, at x = 7.5, 39.5; 71.5, 103.5, 140, 204, and 290 cm (fig. 8). For the rest, the calculation was as before. Figure 9 shows the shear stress distributions. Figure 10 contains the representation of $f(\eta)$. The constant factor in exponents of $f(\eta) = a\, e^{-b \frac{y}{x}}$ disclosed a slight difference from the previous value (fig. 11). But this error was too insignificant to entice us into attempting to express both processes by the same formula (fig. 7). The mean value of b represents the above value 11.16. a again followed at around a = 1, and this value 1 was used thereafter.

Our shear stress distribution formula for flow to rough wall, has thus the same form as for flow from rough to smooth wall, except for the exchange of $\tau_g$ and $\tau_r$:

$$\tau_{(x,y)} = \left[ \tau_g - (\tau_g - \tau_r)\, e^{-11.16 \frac{y}{x}} \right]^{\frac{h-y}{h}} \qquad (4)$$

The same type of shear stress variation testifies to the same type of turbulence.

The extent to which this formula actually represents the experimentally achieved distribution, is shown in figures 4 and 9. In the usually most important region of small x, where transformation advances most rapidly, the assimilation is almost complete; subsequent discrepancies are of much less influence. Concerning the small differences of the experimentally defined shear stress distribution in wall proximity, it may be stated that they are principally due to the fact that the integration constants resulting from the integration of $\int_0^y \frac{1}{\rho} \frac{\partial \tau}{\partial y} dy$ representing the shear stresses on the wall, did not produce exactly identical values. These differences are caused by inaccuracy of measurement and evaluation. In this region the formula seems to reproduce the conditions much better, since the same wall shear stress must prevail.

In retrospect, it may be stated that the above formula reproduces the conditions fairly well and can be used as a basis for computing similar problems. In general, the method of differentiation will have to be resorted to - i.e., start from a known, fully established profile and define $\partial u/\partial x$, exactly as in the first attempted solution - this time with the new shear stress formula - obtaining, according to $u_2 = u_1 + \left(\frac{\partial u}{\partial x}\right)_1 \Delta x$ a new profile. Graphical treatment produces quickest results. The x intervals need not be chosen so very small in order to achieve a good reproduction of the actual curve. In our case, sections of from 10 to 20 cm directly behind the junction point should be chosen, which could even be increased as the spacing is increased.

## SOLUTION OF MOTION EQUATION WITH SIMPLIFIED ASSUMPTIONS

In the following, it is attempted to integrate the motion equation under simplified assumptions by introduction of the shear stress formula. The equation of motion reads:

$$u \frac{\partial u}{\partial x} + v \frac{\partial u}{\partial y} = - \frac{1}{\rho} \frac{\partial p}{\partial x} + \frac{1}{\rho} \frac{\partial \tau}{\partial y} \qquad (5)$$

Our previously obtained formula serves as basis:

$$\tau = \frac{h - y}{h} \left[ \tau_1 + (\tau_2 - \tau_1) e^{-\frac{\alpha y}{x}} \right]$$

$\alpha = 11.16$. $\tau_1$ and $\tau_2$ denote the equilibrium wall shear stress for $x < 0$ and $x = + \infty$.

Now the first simplifying assumption stipulates: $|\tau_2 - \tau_1| \ll \tau_1$. Hence, we can write

$$u(x,y) = u_*(y) + u'(x,y), \qquad v(x,y) = v'(x,y)$$

with $u'$ and $v' \ll U$. $u_*(y)$ is the velocity profile over the roughness 1. With the stream function

$$u' = \frac{\partial \psi}{\partial y}, \qquad v' = - \frac{\partial \psi}{\partial x}$$

while disregarding the small terms $v' \frac{\partial u'}{\partial y}$ and $u' \frac{\partial u'}{\partial x}$, we obtain approximately:

$$u_* \frac{\partial^2 \psi}{\partial y \partial x} - \frac{\partial u_*}{\partial y} \frac{\partial \psi}{\partial x} = - \frac{1}{\rho} \frac{\partial p}{\partial x} + \frac{1}{\rho} \frac{\partial \tau}{\partial y} \qquad (7)$$

With equation (6), the right-hand side assumes the form:

$$- \frac{1}{\rho} \frac{\partial p}{\partial x} - \frac{1}{\rho h} \left[ \tau_1 + (\tau_2 - \tau_1) e^{-\frac{\alpha y}{x}} \right] - \frac{h - y}{\rho h} (\tau_2 - \tau_1) \frac{\alpha}{x} e^{-\frac{\alpha y}{x}}$$

Putting

$$- \frac{1}{\rho} \frac{\partial p}{\partial x} + \frac{1}{\rho} \frac{\partial \tau_1}{\partial y} = - \frac{1}{\rho} \frac{\partial p}{\partial x} - \frac{\tau_1}{\rho h} = f(x)$$

that is, $f(x) = 0$ for $x < 0$, the right-hand side of equation (7) gives:

$$f(x) - \left( \frac{1}{h} + \frac{\alpha}{x} \frac{h - y}{h} \right) (\tau_2 - \tau_1) e^{-\frac{\alpha y}{x}}$$

$$= f(x) - \frac{x + \alpha (h - y)}{h x} (\tau_2 - \tau_1) e^{-\alpha y / x}$$

For medium $x$ and not unusually great $y$, $\alpha(h - y) \gg x$ for $x = \alpha y$, the expression is

$$\frac{x + \alpha(h - y)}{h\ x} = \frac{\alpha}{x}$$

which is to serve as mean value in the subsequent calculation. This comprises the most usually interesting region ($x = 11\ y$). The velocity distribution $u_*$ itself is to be represented by an intervening straight line: $u_* = A + By$. The selection of this straight line should be such as to assure its close approximation to the velocity profile in the pertinent region.

Substituting $v$ for $-\frac{\partial \psi}{\partial x}$ and posing for abbreviation for the constant value, $\frac{\tau_a - \tau_1}{\rho} = C$, equation (7) gives

$$-(A + By)\frac{\partial v}{\partial y} + Bv = f(x) - \frac{\alpha}{x} C\ e^{-\alpha y x} \qquad (8)$$

This is a linear inhomogeneous differential equation of the first order, which is solved by the method of variation of constants. The solution leaves:

$$-v = (A + By)\int_0^y \frac{f(x) - \frac{\alpha}{x} C\ e^{-\alpha\ y/x}}{(A + By)^2}\, dy \qquad (9)$$

The integration constant is zero, since on the wall, that is, for $y = 0$, $v$ must equal zero. The condition of continuity on the other wall is met by means of $f(x)$.

For the further treatment of the above integral $\frac{1}{(A + By)^2}$ is developed by binomial expansion, whereby only the first two terms are considered. Thus

$$\frac{1}{(A + By)^2} = \frac{1}{A^2}\left(1 - \frac{2\ By}{A}\right)$$

and therefore

$$-v' = \frac{(A + By)}{A^2}\int_0^y \left[f(x) - \frac{\alpha}{x} C\ e^{-\alpha\ y/x}\right]\left(1 - \frac{2\ By}{A}\right) dy \qquad (10)$$

The integration affords

$$-v' = \frac{A+By}{A^2}\left[f(x)\left(y-\frac{B}{A}y^2\right)+C\,e^{-\frac{\alpha y}{x}}\left(1-\frac{2B}{A}y-\frac{2B}{A}\frac{x}{\alpha}\right)+2\frac{BC}{A}\frac{x}{\alpha}-C\right] \tag{11}$$

whence the continuity equations give the velocity $u$ at

$$u = -\int_0^x \frac{\partial v}{\partial y}\,dx + u_*$$

In conformity with the initial condition: $x = 0$, $u = U$, the integration constant must be equal $U$. Consequently, $-v'$ must be differentiated again with respect to $y$ and then integrated with respect to $x$, which finally leads to the integral logarithm and, after intermediary calculations:

$$u = \frac{B\,C}{A^2}\left[\frac{B}{A\,\alpha}x^2 - x\right]$$
$$+\left[\frac{1}{A}-\frac{3\,B^2}{A^3}y^2\right]\int_0^x f(x)\,dx + x\,e^{-\frac{\alpha y}{x}}\left[\frac{B\,C}{A^2}-\frac{B^2\,C}{A^3}\left(\frac{x}{\alpha}+y\right)\right]$$
$$-\int_{1/x}^{\infty}\frac{e^{-\alpha y z}}{z}\,dz\left[\frac{C\alpha}{A}-\frac{3\,B^2C}{A^3}\,\alpha\,y^2\right]+u_* \tag{12}$$

$z = \frac{1}{x}$ was chosen as a substitute. Since the integral logarithm produced is tabulated, the problem may be considered solved. The integral logarithm is usually expressed (see Jahnke-Emde) by:

$$\int_x^{\infty}\frac{e^{-t}}{t}\,dt = -E_i(-x) \tag{13}$$

which, in our case, gives:

$$\int_{1/x}^{\infty} \frac{e^{-\alpha y z}}{z}\, dz = -E_i\left(-\frac{\alpha y}{x}\right) \qquad (14)$$

In this manner it is possible to compute, by known wall shear stresses, every profile formed on transition to $\tau_2$, starting from a velocity profile formed over $\tau_1$. We proceeded from the premise that $|\tau_2 - \tau_1| \ll \tau_1$. It should, however, be equally of interest to apply this calculation once for our experimentally explored case, notwithstanding that the assumptions are not completely satisfied and discrepancies therefore may be expected.

The initial profile was that shown in figure 12. The intervening straight line serving as a basis of the calculation is chosen so as to assure comparatively good agreement in the lower region of the velocity profile. Surprisingly, there is a fairly close accord with the measured velocity profiles for small $y$. At greater wall distances the differences are considerable. Above all, the overlapping of two consecutive profiles does not appear. The effected omissions are evidently too great. The principal reason probably lies with the inadmissibility of binomial expansion of $\frac{1}{(A + By)^2}$ for great distances, since the series converges only for $\left|\frac{By}{A}\right| < 1$. Even the approach to 1 causes serious falsification of the result through exclusive consideration of the first two terms. Aside from that, there is also the ommission in the friction terms.

More accurate results, to be sure at greater expense of time and labor, are obtained if the complete friction formula is allowed for in the integration of the above differential equation and $\frac{1}{A^2\left(1 + \frac{By}{A}\right)^2}$ alone is, as before, introduced in the calculation through the first two terms in the binomial expansion. This omission is inevitable if the calculation is to be at all feasible. The solution is:

$$u = -\frac{B\,C}{A^2}\left[\frac{B}{A\,\alpha}\,x^2 - x\right] + \left[\frac{1}{A} - \frac{3\,B^2}{A^3}\,y^2\right]\int_0^x f(x)\,dx$$

$$+ x\,e^{-\alpha\,y/x}\left[\frac{B\,C}{A^2} - \frac{B^2 C}{A^3}\left(\frac{x}{\alpha} + y\right)\right] - \int_{-1x}^{\infty} \frac{e^{-\alpha y z}}{z}\,dz\left[\frac{C\,\alpha}{A}\right.$$

$$\left. - \frac{3\,B^2\,C}{A^3}\,\alpha\,y^2\right] + U + \int_{1/x}^{\infty} \frac{e^{-\alpha y z}}{z}\,dz\left[\frac{2\,C\,\alpha y}{h\,A} - \frac{BC\alpha y^2}{h\,A^2} - \frac{14B^2C\,\alpha y^3}{3h\,A^3}\right]$$

$$+ e^{-\frac{\alpha y}{x}}\left[\frac{B^2\,C}{h\,A^3}\left(\frac{8}{3}\,xy^2 + \frac{7}{3}\,\frac{x^2 y}{\alpha} + \frac{2}{3}\,\frac{x^3}{\alpha^2}\right) - \frac{C}{h\,A}\,x\right] - \frac{2\,B^2 C}{3\,h\,\alpha^2\,A^3}\,x^3$$

(15)

Following this, the velocity for $x = 40$, $y = 1$ was computed as a check on the calculation. The difference from the result obtained with equation (12) was very small as the effect of the additive terms of the last equation does not become noticeable before $x \neq \alpha y$. For the region $x = \alpha y$, equation (12) was quite accurately applicable. Greater $y$ values are, of course, again excluded, because the binomial expansion is then no longer admissible.

In order, therefore, to include this region of greater $y$ values as well, it was attempted to replace the earlier oblique intervening straight line of the velocity distribution by a distribution $U = \text{const}$, that is, by a vertical straight line, and the choice fell to the average velocity $\bar{u} = 1390$ cm/s. The degree of the differential equation was lowered hereby.

From equation (7) follows:

$$u_* \frac{\partial^2 \psi}{\partial y \partial x} = -\frac{1}{\rho}\frac{\partial p}{\partial x} + \frac{1}{\rho}\frac{\partial \tau}{\partial y} = f(x) + \left(\frac{\alpha y}{xh} - \frac{\alpha}{x} - \frac{1}{h}\right) C\,e^{-\alpha\,y/x}$$

(16)

We find

$$u_* = A, \quad u' = \frac{\partial \psi}{\partial y}, \quad v' = -\frac{\partial \psi}{\partial x}$$

Therefore

$$\frac{\partial \psi}{\partial x} = -v' = \frac{1}{A}\int_0^y \left[ f(x) + \left( \frac{\alpha y}{xh} - \frac{\alpha}{x} - \frac{1}{h} \right) C\, e^{-\alpha\, y/x} \right] dy$$

With the aid of the continuity, we obtain for u:

$$u = \frac{1}{A}\int_0^x \left[ f(x) + \frac{e^{-\alpha\, y/x}}{x} \left( \frac{Cy\alpha}{h} - C\,\alpha \right) - \frac{C}{h} e^{-\alpha\, y/x} \right] dx + u_* = u' + u_* \tag{17}$$

where $u_*$ denotes the initial profile and $u'$ the additional velocity.

With $\frac{1}{x} = z$ chosen as substitution, the integration gives

$$u' = \frac{1}{A}\int_0^x f(x)\,dx + \left( \frac{2C\alpha y}{Ah} - \frac{C\alpha}{A} \right) \int_{1/x}^{\infty} \frac{e^{-\alpha y z}}{z}\, dz - \frac{C\,x}{A\,h}\, e^{-\alpha\, y/x} \tag{18}$$

The velocity profiles were computed for x = 20, 40, 70, 150, and 290 cm distance. A comparison of these results with the experimental velocity distributions surprisingly disclosed a relatively good agreement, especially in the middle of the channel (fig. 13). The overlapping of the theoretical profiles already occurs at smaller y values, so that here the departure is somewhat greater. In direct proximity of the wall the calculation is inapplicable because the integral logarithm

$$-E_i\left(-\frac{\alpha\, y}{x}\right) = -E_i(0)$$

becomes infinite.

To achieve a closer approach to reality, the profile could now be replaced in the lower region by an oblique, in the middle by a vertical straight line. A stepped distribution would also be feasible, special considerations being then necessary on the points of discontinuity of the

velocities. A comparison of such results with the experiment would surely be interesting. Yet another profitable study should be the extent to which the shear stress formula obtained above holds true in a comparison with the actual processes under entirely dissimilar types of roughness.

Translation by J. Vanier,
National Advisory Committee
for Aeronautics.

## REFERENCES

1. Prandtl, L.: Recent Results of Turbulence Research. T.M. No. 720, NACA, 1933.

   Nikuradse, J.: Strömungsgesetze in rauhen Rohren. Forsch.-Arb. d. Ing.-Wes., Heft 361, Berlin 1933.

   Hopf, L.: Die Messung der hydraulischen Rauhigkeit. Z.f.a.M.M., vol. 3, no. 5, Oct . 1923, p. 329.

   Fromm, K.: Strömungswiderstand in rauhen Rohren. Z.f.a.M.M., vol. 3, no. 5, Oct. 1923, pp. 339-358.

2. Roux, L.: Zeitschrift für Geophysik 1935.

3. Motzfeld, H.: Die turbulente Strömung an welligen Wänden. Dissertation Göttingen 1935. Z.f.a.M.M., vol. 17, no. 4, Aug. 1937, pp. 193-212.

4. Kirsten: Dissertation, Leipzig, 1927.

5. Prandtl, L.: Zur Berechnung der Grenzschichten. Z.f.a.M.M., vol. 18, no. 1, Feb. 1938, pp. 77-82.

6. Prandtl, L.: Turbulent Flow. T.M. No. 435, NACA, 1927.

7. Schlichting, H.: Experimental Investigation of the Problem of Surface Roughness. T.M. No. 823, NACA, 1937.

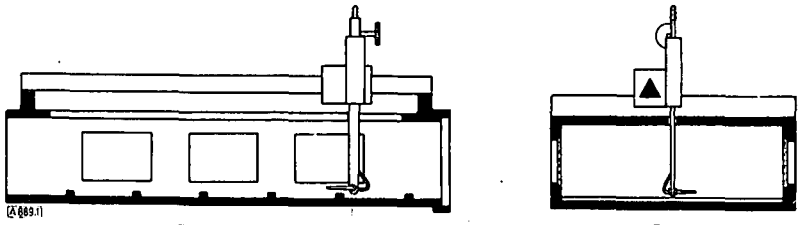

Figure 1.- View of test channel.

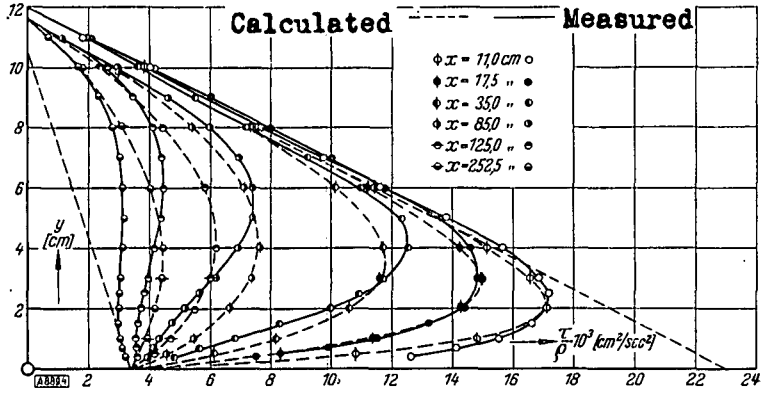


Figure 4.- Shear stress distribution on transition from rough to smooth wall.

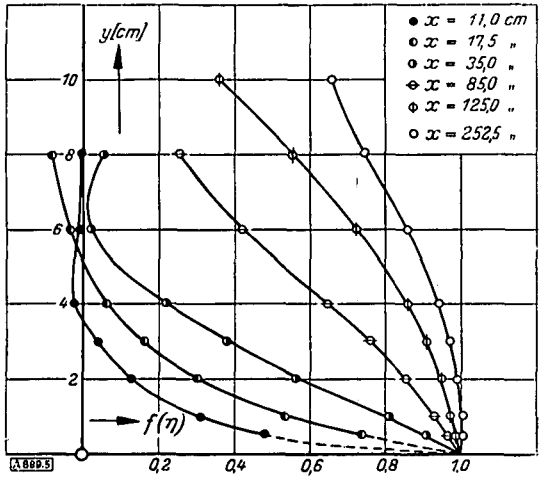


Figure 5.- f(η) plotted against wall distance y for different parameters x. (from rough to smooth)

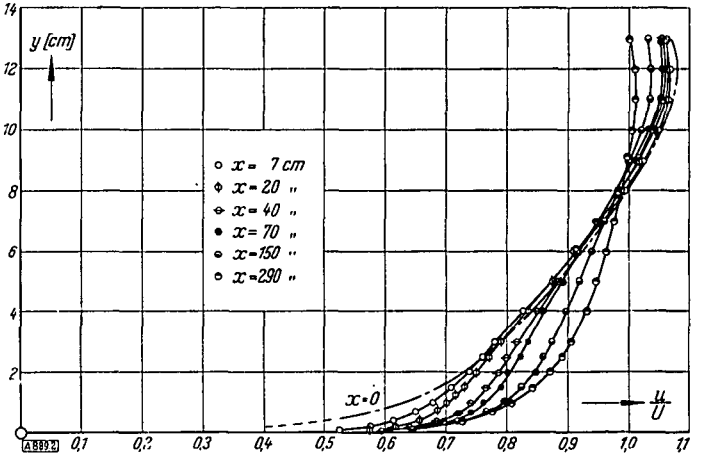


Figure 2.- Velocity profiles on transition from rough to smooth wall. x=distance from last roughness.

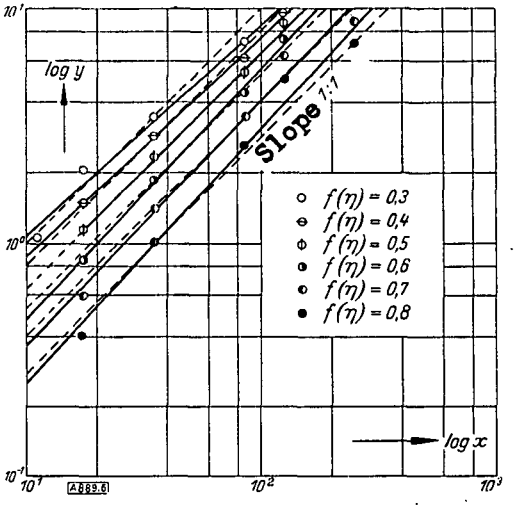


Figure 6.- Log y plotted against log x for different $f(\eta)$ $a \cdot e^{-by/x^m}$ const. for defining exponent m from the slope of the curves. (from rough to smooth)

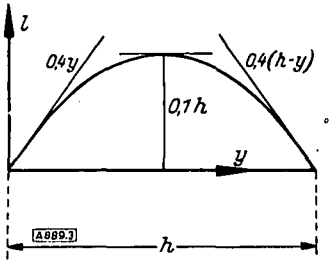


Figure 3.- Sketch of assumed mixing path distribution.

Figs. 1,2,3,4,5,6.

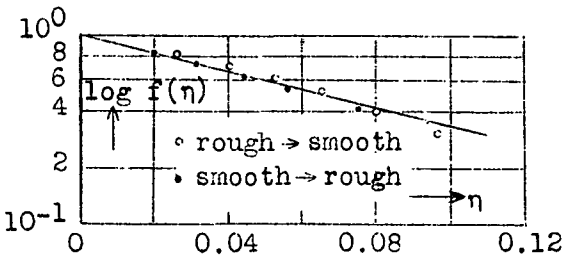


Figure 7.- Determination of a and b.

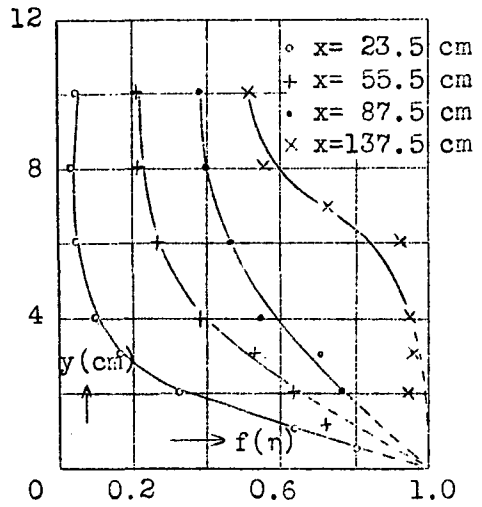


Figure 10.- f(η) plotted against wall distance y for different parameters x. (smooth to rough)

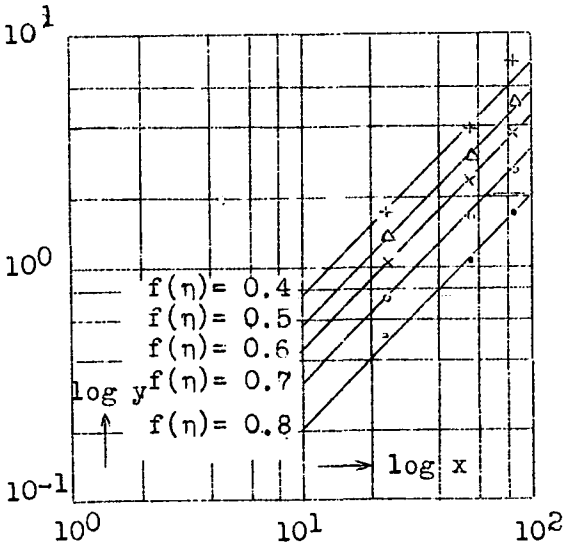


Figure 11.- Determination of exponent m for transition from smooth to rough.

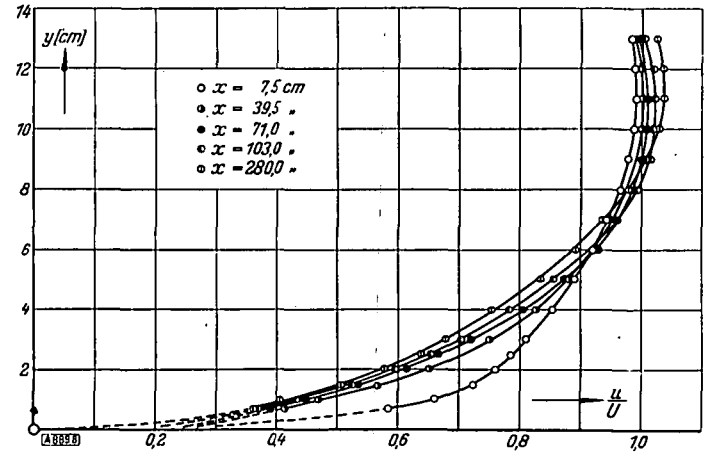


Figure 8.- Velocity distributions on transitions from smooth to rough.

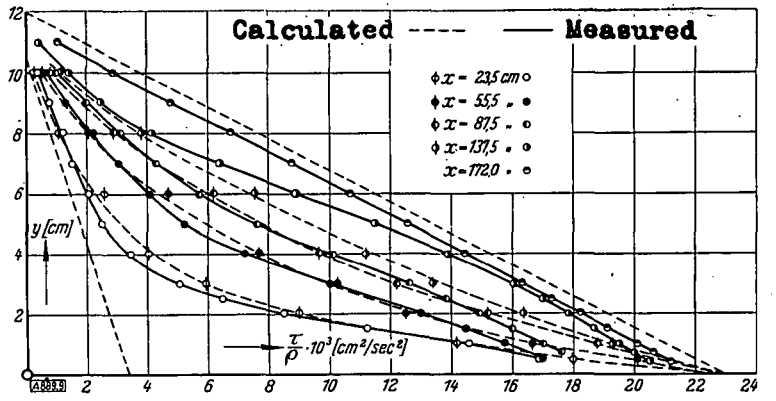


Figure 9.- Shear stress distribution on transitions from smooth to rough.

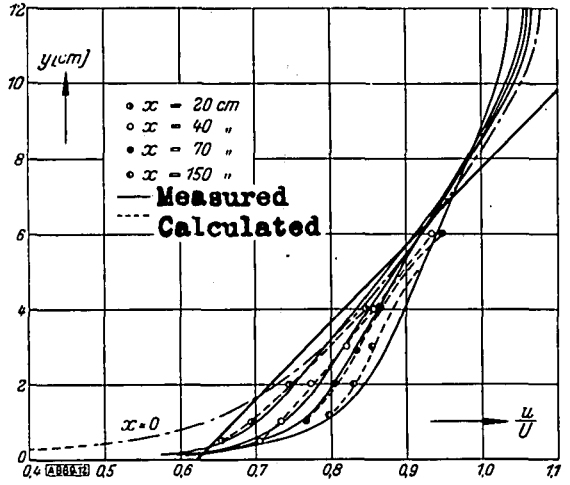


Figure 12.- Comparison of calculated and measured velocity distributions on the basis of the oblique intervening straight line.

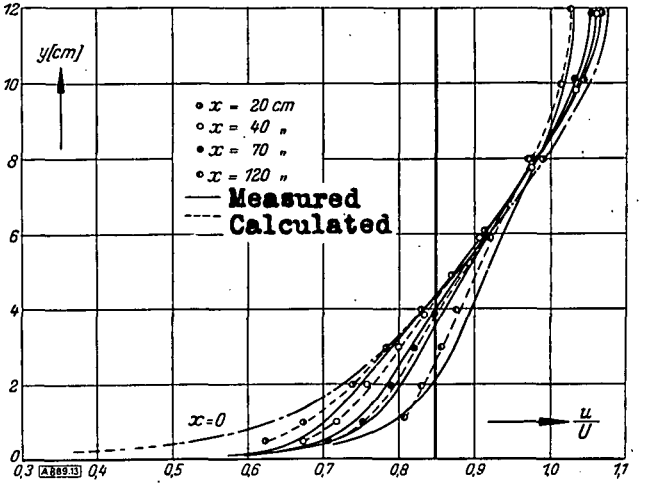


Figure 13.- Comparison of computed and measured velocity distributions, the calculations being based on a velocity distribution $\frac{u}{U}=0.85$ constant over the section.

Figs. 8,9,12,13.